Atmos. Chem. Phys. Discuss., 8, 20155–20192, 2008
www.atmos-chem-phys-discuss.net/8/20155/2008/

Atmospheric Chemistry and Physics Discussions

This discussion paper is/has been under review for the journal *Atmospheric Chemistry and Physics (ACP)*. Please refer to the corresponding final paper in *ACP* if available.

An evaluation of the simulation of the edge of the Antarctic vortex by chemistry-climate models

H. Struthers[1], G. E. Bodeker[1], J. Austin[2], S. Bekki[3], I. Cionni[1], M. Dameris[4], M. A. Giorgetta[5], V. Grewe[4], F. Lefèvre[3], F. Lott[6], E. Manzini[7,8], T. Peter[9], E. Rozanov[9,10], and M. Schraner[9]

[1]National Institute of Water and Atmospheric Research, Lauder, New Zealand
[2]Geophysical Fluid Dynamics Laboratory, NOAA, Princeton, New Jersey, USA
[3]Service d'Aeronomie du CNRS, Institut Pierre-Simon Laplace, Paris, France
[4]Institut für Physik der Atmosphäre, Deutsches Zentrum für Luft- und Raumfahrt, Oberpfaffenhofen, Wessling, Germany
[5]Max Planck Institut für Meteorologie, Hamburg, Germany
[6]Laboratoire de Meteorologie Dynamique, Paris, France
[7]Istituto Nazionale di Geofisica e Vulcanologia, Italy

[8] entro Euro-Mediterraneo per i Cambiamenti Climatici, Bologna, Italy
[9] Institute for Atmospheric and Climate Science ETH, Zurich, Switzerland
[10] PMOD/WRC, Dorfstrasse 33, 7260, Davos Dorf, Switzerland

Received: 17 September 2008 – Accepted: 7 October 2008 – Published: 1 December 2008

Correspondence to: H. Struthers (h.struthers@niwa.co.nz)

Published by Copernicus Publications on behalf of the European Geosciences Union.

Abstract

The dynamical barrier to meridional mixing at the edge of the Antarctic spring stratospheric vortex is examined. Diagnostics are presented which demonstrate the link between the shape of the meridional mixing barrier at the edge of the vortex and the meridional gradients in total column ozone across the vortex edge. Results derived from reanalysis and measurement data sets are compared with equivalent diagnostics from five coupled chemistry-climate models to test how well the models capture the interaction between the dynamical structure of the stratospheric vortex and the chemical processes occurring within the vortex. Results show that the accuracy of the simulation of the dynamical vortex edge varies widely amongst the models studied here. This affects the ability of the models to simulate the large observed meridional gradients in total column ozone. Three of the models in this study simulated the inner edge of the vortex to be more than 7° closer to the pole than observed. This is expected to have important implications for how well these models simulate the extent of severe springtime ozone loss that occurs within the Antarctic vortex.

1 Introduction

Models capable of simulating the most important processes involved in the production and destruction of stratospheric ozone are critical tools for increasing our understanding of variations in the stratospheric ozone layer and predicting the consequences of anthropogenic emissions of ozone depleting substances. Two dimensional (latitude-altitude), zonally averaged models of composition, dynamics and radiation have been extensively used to estimate the evolution of the ozone layer and to predict future stratospheric change (Hofmann et al., 1999; Chipperfield et al., 2003; Chipperfield and Feng, 2003). However, two-dimensional models are not capable of adequately representing the ozone distribution in the polar regions (Chipperfield et al., 2003).

Three dimensional coupled chemistry-climate models (CCMs), designed to include

ACPD

8, 20155–20192, 2008

representations of dynamical, radiative, and chemical processes in the atmosphere and their interactions are now being routinely used for the projections of future stratospheric change (Austin and Wilson, 2006; Eyring et al., 2007; Gettelman et al., 2008). To have confidence in CCM projections of future ozone recovery as the provisions of the Montreal Protocol and its amendments lead to the removal of halogens from the stratosphere, it is necessary to rigourously assess the reliability of CCMs. One method for evaluating such models is to simulate the past evolution of ozone, other trace gas species and dynamics under the varying natural and anthropogenic forcings, and compare such simulations with observations. Such comparisons not only highlight model deficiencies, but can help improve our understanding of processes, mechanisms and feedbacks within the atmosphere. This is the motivation behind the CCMVal (Chemistry Climate Model Validation, Eyring et al., 2005) activity of the SPARC (Stratospheric Processes and their Role in Climate) project of WCRP (World Climate Research Programme). Within the CCMVal project, the aim is to characterize the simulation of atmospheric processes in CCMs and their associated General Circulation Models (GCMs) using a process-oriented approach to model validation.

How well CCMs simulate dynamical fields at the edge of the Antarctic polar vortex is important for the accurate simulation of ozone concentrations at high southern latitudes. This is because the mixing barrier at the edge of the vortex determines how well air within the vortex is isolated from mid-latitude air. This isolation is critical for the development of the Antarctic ozone hole (Juckes and McIntyre, 1987; Schoeberl and Hartmann, 1991; Solomon, 1999). Modeled ozone in the polar region is therefore sensitive to the simulation of the dynamical vortex. For example, Kinnison et al. (2007) show that the amount of active chlorine within the Antarctic vortex simulated by the MOZART-3 chemistry transport model, depended on the transport and the degree of isolation of the vortex.

The primary objective of this paper is to evaluate the ability of five CCMs to simulate the position of the mixing barrier at the edge of the Antarctic polar vortex and the associated latitudinal gradient in ozone concentration across this barrier. Mixing barriers

at the edge of the polar winter vortices have been quantified through Lagrangian transport studies (Bowman, 1993; Manney et al., 1994; Paparella et al., 1997; Günther et al., 2007), contour advection (Chen, 1994), effective diffusivity (Haynes and Shuckburgh, 2000; Allen and Nakamura, 2001) and, in a recent paper Krützmann et al. (2008) use Rényi entropy to diagnose the mixing barrier at the edge of the Antarctic vortex as simulated in the SOCOL (Egorova et al., 2005) CCM. In this work, the meridional impermeability (κ) defined by Bodeker et al. (2002) (also see Sect. 2) is used to diagnose the position and strength of the mixing barrier at the vortex edge. κ has been used to diagnose vortex isolation by Tilmes et al. (2006) as part of a study to quantify chemical ozone loss during the setup phase of the polar vortex.

Wang et al. (2005) compared results from a Lagrangian particle model, a contour advection model and a vortex edge diagnostic very similar to κ. They show using contour advection, that there is a distinct minimum in the growth of total contour numbers across the polar jet indicating that the polar jet is effectively separating air particles inside the vortex from those outside the vortex. The position, in equivalent latitude coordinates of the minimum of the growth of total contour numbers coincides with the peak of the vortex edge diagnostic (κ diagnostic).

Bodeker et al. (2002) (hereafter referred to as B2002) used equivalent latitude zonal means of ozone and meteorological reanalysis to study the expansion of the Antarctic ozone hole and its encroachment on the observed edge of the vortex. They used equivalent latitude coordinates to remove the effects of vortex displacement and elongation which tend to blur gradients near the vortex edge when taking zonal means in true latitude coordinates.

B2002 demonstrated that while the size of the vortex and the area where temperatures fall below 195 K changed little from 1980 to 2000, the area with ozone below 220 Dobson Units (DU), the contour defining the ozone hole, steadily increased. Over the 20 year period (1981–2000), the severity of the ozone depletion within the core of the vortex also increased. The study of B2002 is extended here to show an additional five years of results. Results from observations and meteorological reanalysis are used

as context for the examination of how well five coupled chemistry-climate models capture the features of the dynamical vortex and the effect this has on the modeled ozone distribution, in particular the models' representation of the Antarctic ozone hole.

2 Measurement data sets and vortex diagnostics

The ozone measurements used in this study were taken from the NIWA combined total column ozone data-base (Bodeker et al., 2005) which is an update of the data-base used in B2002. The data-base combines satellite-based ozone measurements from four Total Ozone Mapping Spectrometer (TOMS) instruments, three different retrievals from the Global Ozone Monitoring Experiment (GOME) instruments, and data from four Solar Backscatter Ultra-Violet (SBUV) instruments. Comparisons with the global ground-based World Ozone and Ultraviolet Data Center (WOUDC) Dobson spectrophotometer network have been used to remove offsets and drifts between the different data sets to produce a global homogeneous total ozone column data-set that combines the advantages of good spatial coverage of satellite data with the long-term stability of ground-based measurements. Updated versions of the TOMS (version 8), GOME (version 3.1) and SBUV (version 8) retrieval software, together with assimilated total column ozone fields from Royal Netherlands Meteorological Institute (KNMI), have been used to generate the data set. For more details on the NIWA data-base including a description of the error characteristics of the ozone fields, see Bodeker et al. (2005).

The meridional impermeability, κ is defined as the gradient of potential vorticity (PV) with respect to equivalent latitude (ϕ_e) multiplied by the horizontal wind speed ($|\mathbf{V}|$) on a given potential temperature surface:

$$\kappa = \frac{d\mathrm{PV}}{d\phi_e} \times |\mathbf{V}| \tag{1}$$

Wind, temperature and PV fields on potential temperature surfaces were taken from NCEP/NCAR reanalyses (Kistler et al., 2001). κ is a purely dynamical construct, rather

than being defined based on the distribution of an advected tracer. It can therefore be calculated directly from meteorological reanalyses and compared with the same diagnostic calculated from CCM or GCM output. Meridional transects of equivalent latitude zonal mean κ versus equivalent latitude highlight the position and latitudinal structure of the meridional mixing barrier at the vortex edge (Wang et al., 2005).

Daily NCEP/NCAR PV fields (2.5° latitude×2.5° longitude resolution) on the 550 K potential temperature surface were used to define the equivalent latitude coordinate (Bodeker et al., 2005). The 550 K potential temperature surface was chosen for the derivation of equivalent latitudes and κ because, for high latitude total column ozone, it is close to the altitude of the maximum in the ozone number density (Vincent and Tranchant, 1999). Daily PV versus equivalent latitude zonal means were generated and these were used to transform the ozone and temperature fields to a equivalent latitude coordinate. The same procedure was used to generate equivalent latitude zonal mean results from the models.

3 CCM descriptions

All of the models shown here are fully coupled CCMs that include representations of the feedbacks between the dynamics, radiation and chemistry which are present in the real stratosphere. In particular, the way the models simulate the dynamical vortex will impact the in-situ chemistry which can feed back to the dynamics through changes in the distribution of radiatively active gases.

A short summary of the essential characteristics of each model is given in Table 1. All of the models have been validated against measurements and intercompared with other CCMs (Eyring et al., 2006, 2007; Bodeker et al., 2007; Austin et al., 2008). The models shown here are a subset of all the models participating in CCMval. Only groups that submitted daily PV, wind and total column ozone model output to the CCMval archive are included in this study.

E39C-A (Stenke et al., 2008a,b) is an upgraded version of the CCM E39C (Dameris

et al., 2005, 2006) employing the fully Lagrangian advection scheme ATTILA (Reithmeier and Sausen, 2002) for tracer transport. ATTILA is strictly mass conserving and numerically non-diffusive. Water vapor, cloud water and chemical trace species are advected by ATTILA instead of the operational semi-Lagrangian advection scheme of Williamson and Rasch (1994) which has been used in the previous model version E39C.

Extensive changes have been made to the chemistry and advection schemes in the SOCOL model (Schraner et al., 2008) from that presented in Eyring et al. (2006); Bodeker et al. (2007); Eyring et al. (2007); Austin et al. (2008). Results from SOCOL version 2.0 are used in this study.

The underlying GCM used in the MAECHAM4CHEM and SOCOL models is the middle atmosphere configuration of ECHAM4 (MAECHAM4) (Manzini et al., 1997). One notable difference in the way the MAECHAM4 is configured in MAECHAM4CHEM and SOCOL is that the non-orographic gravity wave scheme in SOCOL has been modified to produce slightly stronger non-orographic gravity wave drag than MAECHAM4CHEM. This adjustment results in some improvements to the dynamical representation of the stratosphere in SOCOL with respect to MAECHAM4CHEM (see Figs. 1, 2 and 3 of Eyring et al., 2006).

The chemistry scheme in UMETRAC has been updated since Austin (2002) and is now the same as the scheme used in the AMTRAC model (Austin and Wilson, 2006). Model results in the rest of this paper are listed in alphabetical order.

All models use the same prescribed changes in ozone depleting substances, well mixed greenhouse gases and stratospheric aerosol surface area densities as well as observed sea surface temperatures and sea ice lower boundary conditions. These boundary conditions are the same as those used in the so called REF1 CCMVal integrations described in detail in Eyring et al. (2006).

4 Dynamical containment of ozone depletion diagnosed in measurements

Antarctic ozone depletion usually maximizes during early October (Bodeker et al., 2005). Figure 1 shows the equivalent latitude zonal mean, October average of daily mean total column ozone, κ and 550 K temperature averaged over five year periods This extends Figs. 2 and 4 of B2002 for a further 5 years.

The total ozone column zonal mean (Fig. 1a) demonstrate that the severity of Antarctic ozone depletion increased from 1981 to 2000 as indicated by the steady decline in the total column ozone poleward of the vortex edge (>62° S). In conjunction with the increased severity of ozone depletion, the equivalent latitude at which the contours cross the 220 DU threshold (denoted by the horizontal dashed line in Fig. 1a) steadily decreased from 1981 to 2000 indicating an increase in area of the ozone hole. These trends reverse for the 2001/2005 five year average where the average total column ozone within the vortex is more than 20 DU greater than the previous five year average and the equivalent latitude poleward of which ozone drops below 220 DU has moved poleward by approximately four degrees.

The reversal of the ozone trend is not necessarily an indication of the recovery of Antarctic ozone from the effect of reductions in stratospheric halogen concentrations. The severity of ozone depletion within the Antarctic polar vortex for a given spring, depends on both chemical and dynamical conditions (Huck et al., 2005). The 2002 to 2005 period was significantly more dynamically active and stratospheric temperatures were higher than normal. This can be seen in the 550 K temperature plot (Fig. 1c) where the 2001/2005 five year average within the polar vortex is higher by at least 2 K compared with the other five year averages and more than 4 K higher when compared with the previous five year average (1996/2000). The 2001/2005 averages are also strongly affected by the unprecedented 2002 Antarctic sudden stratospheric warming (Hoppel et al., 2003; Sinnhuber et al., 2003; Nishii and Nakamura, 2004; Randall et al., 2005).

Changes similar to the total column ozone changes in Fig. 1a can also be seen

ACPD
8, 20155–20192, 2008

in the meridional impermeability, κ (Fig. 1b) derived from NCEP/NCAR reanalyses. Peak κ increased by more than 50% from 1980 to 2000. As pointed out in B2002, no secular trend in the equivalent latitude position of the peak in κ can be seen in the reanalysis results, indicating that there has been no change in the size of the dynamical vortex even though there were significant increases in the peak κ, an indicator of the permeability of the vortex edge, and the size of the ozone hole over the same period.

The 550 K temperatures (Fig. 1c) from NCEP/NCAR reanalysis data show a cooling trend in the tropics for equivalent latitudes less that 20° S (equivalent to a shift to lower pressures of the 550 K potential temperature surface). Compared to the 1981/1985 average, tropical temperatures on the 550 K surface were almost 3 K lower over the 2001/2005 period. Within the polar vortex the results of Fig. 1c indicate temperatures increased over the 25 year period from 1980 to 2005, with the 1995/2000 average being anomalously low. Cooling in the tropics and warming at high latitudes in the lower stratosphere is consistent with an increase in the strength of the Brewer-Dobson circulation (Butchart et al., 2006).

The edge of the polar vortex can been defined in a number of ways (Bodeker et al., 2002; Nash et al., 1996; Tilmes et al., 2006). Here we define the "vortex edge" as the peak in κ and the "inner vortex edge" as the minimum of the second derivative of κ with respect to equivalent latitude. Figure 2 updates Fig. 3 of B2002, and shows for each year the October average equivalent latitude of the 220 DU total column ozone contour, the equivalent latitude of the vortex edge and the inner vortex edge. The difference between the edge of the ozone hole (220 DU contour) and the vortex edge decreased from 1980 to the early 1990s and remained relatively constant around 4 to 5 degrees from 1990 to 2005. There is a suggestion that this gap between the vortex edge and the 220 DU contour started to widen after 2000 but the 2005 ozone hole edge closed to within 2.5° of the vortex edge.

The equivalent latitude of the 220 DU total column ozone contour closely tracks the equivalent latitude of the inner vortex edge after 1990. This demonstrates how the area of severe ozone depletion within the vortex expanded to the edge of the vortex over the

ACPD
8, 20155–20192, 2008

1980 to 1990 period. After 1990 the ozone hole has not grown any larger relative to the inner vortex edge (Fig. 2b) which implies the size of the ozone hole has largely been constrained by the size of the dynamical vortex over the 1990 to 2005 period.

Both the vortex edge and the inner vortex edge time-series (Fig. 2a) show no change in their respective equivalent latitude position from 1980 to 2005 in response to the growth in the ozone hole. Therefore the position and width of the vortex edge and thus the size of the dynamical vortex is insensitive to the concentration of ozone within the vortex.

5 Dynamical containment of ozone depletion simulated by five CCMs

For the comparison between observations/reanalysis and models, the 1990 to 2000 period was chosen because after approximately 1990, the equivalent effective stratospheric chlorine (EESC) (Newman et al., 2004) remained relatively constant. This means that after 1990, the variability in the severity of springtime Antarctic ozone losses has primarily been driven by dynamical variability and chemical/radiative/dynamic coupling rather than through significant changes in EESC (Huck et al., 2005) (see also Fig. 2). Most of the model simulations used in this work finish in 2000 so this was taken as the end point of the averaging period.

5.1 Modeled meridional impermeability

Figure 3 plots the 10 year average (1990–1999) of the equivalent latitude zonal mean κ derived from NCEP/NCAR reanalyses and from the five CCMs. The dominant feature in the κ equivalent latitude zonal means, the peak spanning the vortex edge at approximately 62° S, is reproduced by all of the CCMs but the details are not well simulated by some of the models.

E39C-A, E39C, LMDZrepro and UMETRAC have vortex edge barriers that are significantly too wide. The equivalent latitude of the vortex edge, as simulated by E39C-A,

ACPD
8, 20155–20192, 2008

E39C and LMDZrepro are in good agreement with reanalysis results but because the edge barrier is too wide, the inner vortex edge is too close to the pole.

Comparisons of the κ equivalent latitude zonal means from E39C-A and E39C provide information on the influence on κ of changes in the trace gas advection scheme. κ from both models are similar with the E39C-A showing a small improvement compared to reanalysis on the equatorward side of the κ peak.

The inner edge of the vortex in MAECHAM4CHEM agrees well with the reanalysis results. A second smaller κ peak within the vortex is apparent in the MAECHAM4CHEM results (Fig. 3d). This feature is associated with small, high PV events that occur early in October within the polar vortex in some years. These features are also present to a lesser degree in the SOCOL fields (Fig. 3e) suggesting that they are generated by the underlying MAECHAM4 GCM. The cause of these features is presently not clear. The 1σ range in κ from SOCOL is the only model result to capture the mean κ from reanalysis over the whole latitude range spanning the vortex edge.

The shape of the κ peaks from MAECHAM4CHEM and SOCOL are similar. MAECHAM4CHEM and SOCOL are constructed using the same underlying GCM (MAECHAM4). The similarity of the κ zonal means from MAECHAM4CHEM and SOCOL and the insensitivity of κ to changes in advection scheme (E39C-A/E39C) demonstrate that the shape of the κ peak derived from CCM output is strongly related to the underlying dynamical model rather than the chemistry or spatial distribution of radiatively active gases. This is consistent with the results in Sect. 4 which show the position and width of the κ peak in the reanalysis data did not significantly change over the 26 year period 1980–2005, even though the concentration of ozone within the polar vortex declined markedly over the same period.

UMETRAC generates a vortex edge barrier that is too wide (Fig. 3f). The vortex edge is closer to the pole than reanalysis and this, combined with the fact that the vortex barrier is too wide means that the inner vortex edge is significantly too close to the pole.

The Arctic and Antarctic meridional impermeability simulated by the WACCM3 CCM

(Tilmes et al., 2007) have been compared to the κ calculated using the UK Meteorological office stratospheric analyses (Swinbank and O'Neill, 1994) for the period 1992 to 2003. The WACCM3 model produces an October average meridional impermeability (κ) whose shape is similar to the LMDZrepro results shown here (see Fig. 5 of Tilmes et al., 2007). The position of the peak of the WACCM3 κ zonal mean matches reasonably well the peak derived from the Meteorological Office analyses but the peak is too low and significantly too broad. Note also the shape of the κ zonal means from the Meteorological Office analyses shown in Tilmes et al. (2007) are in good agreement with the κ results derived from NCEP/NCAR reanalyses shown here. The absolute values of κ from Tilmes et al. (2007) differ with results presented here because they used modified PV in their study, whereas Ertel PV is used here.

To quantify the shapes of the κ zonal means, the first three moments of κ were fitted over a limited latitude range around the vortex edge peak:

$$m_1 = \int_a^b \phi_e \kappa(\phi_e) d\phi_e$$

$$m_2 = \int_a^b (\phi_e - m_1)^2 \kappa(\phi_e) d\phi_e$$

$$m_3 = \int_a^b \left(\frac{(\phi_e - m_1)}{m_2} \right)^3 \kappa(\phi_e) d\phi_e.$$

Table 2 lists the fitted coefficients and the latitude range over which the κ values were fitted. A normalizes the functions such that the integral under the original and the fitted curves are equal over the range of latitudes considered. m_1, m_2 and m_3 are the fitted coefficients representing the first, second and third moments respectively. Each year was fitted separately. The 10 year mean of the fitted coefficients are listed in Table 2 along with the 1σ standard deviation in the fitted values.

The m_1 values from E39C-A, LMDZrepro and UMETRAC results are significantly larger than the reanalyses, demonstrating that the vortex edge in these models is too

close to the pole. As discussed above, all models except SOCOL have a κ peak that is too broad compared to reanalyses.

The fitted first and second moments from Table 2 were used to plot the fitted Gaussian functions

$$\kappa_f(x) = \frac{A}{m_2\sqrt{2\pi}} \exp\left(\frac{(x-m_1)^2}{2m_2^2}\right) \quad (2)$$

representing the vortex mixing barrier, shown in red in Fig. 3. If the dynamical barrier is assumed to have a Gaussian shape as in Eq. 2, the inner vortex edge is then simply m_1+m_2. As pointed out above, the MAECHAM4CHEM and SOCOL inner vortex edges agree well with the reanalysis results. The other models (E39C-A, LMDZrepro and UMETRAC) simulate inner vortex edges more than 7 degrees closer to the equivalent latitude pole than the inner vortex derived from reanalyses.

5.2 Modeled total column ozone

There is a sharp decrease in total column ozone at the edge of the vortex from the NIWA observation data set (Fig. 4a) over a limited equivalent latitude range, approximately 60° S–70° S. This large gradient across the vortex edge highlights the advantage of using equivalent latitude coordinates where the effects of distortion and/or displacement of the vortex are reduced compared to true latitude coordinates (Bodeker et al., 2005). Using equivalent latitude rather than true latitude gives a clearer picture of the vortex edge which helps in diagnosing the isolation of inner vortex air. The strong gradient in total column ozone across the vortex edge represents the region over which the inner vortex air, which is depleted in ozone, mixes with ozone rich air from outside the vortex.

The overall magnitude and latitudinal shape of the modeled total column ozone are in reasonable agreement with observations from the NIWA combined total column database (Fig. 4). The LMDZrepro and UMETRAC ozone holes are too deep in the vicinity

ACPD
8, 20155–20192, 2008

of the equivalent latitude pole and the MAECHAM4CHEM ozone columns are positively biased over the whole of the southern hemisphere as noted by Steil et al. (2003).

The E39C-A total columns also have a positive bias over the whole of the southern hemisphere. The shape of the equivalent latitude zonal mean total column ozone (Fig. 4b) is a small improvement compared to results from the E39C model but at the expense of introducing a positive bias at mid and high latitudes. The ozone gradient over the vortex edge is steeper and the large gradients near the vortex edge are more confined in latitude in the E39C-A results compared to E39C results.

Total column ozone results from SOCOL version 2.0 shown here are a significant improvement on the results shown in Eyring et al. (2006, 2007) and are in excellent agreement with observations, particularly in the tropics and high latitudes.

The meridional gradients of total column ozone are closely related to κ. This is clear from Fig. 5 where the κ zonal means are compared to the negative of the gradient of the total ozone column with respect to equivalent latitude, from observations and the five CCMs. The correlation between κ and the gradient in ozone is good in all cases, particularly near the vortex edge.

The 550 K potential temperature surface on which κ are calculated is close to the altitude where the ozone number density maximizes in the polar regions. Even though the total column ozone is an integrated quantity over the full atmospheric column, it is weighted strongly to ozone concentrations around the 550 K level and thus the total column ozone zonal means are related to κ on the 550 K surface. This is confirmed by comparing the total column ozone gradients with gradients in ozone concentration on the 550 K potential temperature surface from the models. The peak gradients at the vortex edge match well.

Figure 5 demonstrates that κ clearly defines the position and structure of the barrier to meridional mixing at the edge of the polar vortex (Wang et al., 2005) and is therefore an important diagnostic for the validation of stratospheric resolving CCMs.

Note that the differences in the model and reanalysis/observed meridional equivalent latitude zonal means are not a result of distortions due to the transformation to

equivalent latitude coordinates. The same conclusions hold when the diagnostics are calculated in true latitude coordinates. κ is the product of wind speed and the potential vorticity gradient. Comparing these fields separately indicates that there is a greater discrepancy between the NCEP/NCAR reanalyses and CCMs in the PV gradients than the wind speed. In particular, the models generally produce larger PV gradients than the reanalysis within the inner vortex. The reason for this discrepancy is presently not clear.

Although it is outside the scope of this paper, the results of this and the previous section raises the question of whether the κ diagnostic along with the total column ozone fields can be used to quantify the ozone transport across the vortex edge during the spring time period of severe ozone loss within the Antarctic polar vortex. This is an attractive goal because it would allow the estimation of ozone transport across the vortex edge directly from standard meteorological output (winds and PV) and total column ozone without the need for any additional Lagrangian (Wang et al., 2005) or tracer origin tagging (Grewe, 2006) model experiments.

Qualitatively, the maximum ozone gradient is correlated with the peak height and the κ gradient (peak height divided by the half width) and inversely correlated with the width of the κ peak (see Table 2). The correlation coefficients, treating each year (1990–1999) separately, are similar for the three κ parameters (peak height, width and κ gradient) with values around 0.5. In the framework of turbulent diffusion, the meridional ozone flux is proportional to the meridional ozone gradient (Vincent and Tranchant, 1999) but it is outside the scope of this study to quantify any relationship between the κ peak and the transport across the vortex edge.

5.3 Vortex edge influence on other atmospheric quantities

The correlation between κ and the total column ozone meridional gradients in Fig. 5 highlights how closely linked the dynamics, transport and chemistry (particularly ozone) are in vicinity of the polar vortex edge. This is reinforced by Fig. 6 which shows the October average, 1990–1999 equivalent latitude zonal mean temperature, ozone,

ClO_X(=Cl+ClO+Cl_2O_2), water vapor and CH_4 mixing ratios and the mean age of stratospheric air (Andrews et al., 2001) on the 550 K potential temperature surface using UMETRAC output as an example. The modeled quantities shown in Fig. 6 represent dynamics (temperature), chemistry (ozone, ClO_X, CH_4 and H_2O), transport (CH_4 and mean age of air) and radiatively active species (ozone, CH_4 and H_2O). The physical process of dehydration within the vortex (Solomon, 1999) is also evident in Fig. 6f. In all cases, the equivalent latitude zonal means of these quantities are intimately related to the position and width of the corresponding κ peak. In some cases (temperature and ozone) the gradients across the vortex edge are prominent over the whole κ peak, in other cases the change occurs in the vicinity of the inner (ClO_X and H_2O dehydration) or outer (mean age and H_2O) edge of the vortex.

The details of these relationships between the dynamical representation of the vortex edge and other atmospheric quantities, the interplay between them, the similarities and differences between the Antarctic and Arctic vortices and how well the current generation of CCMs simulate these compared to the real atmosphere remain open questions but are an important area for future research. New coordinated model runs and new observational data sets (Hassler et al., 2008; Santee et al., 2008) should be of use in helping to address these questions.

5.4 The growth and dynamical containment of Antarctic ozone depletion

The results presented in the above sections point to weaknesses in the dynamical simulation by CCMs of the Antarctic polar vortex and the spring time chemical ozone loss within the vortex. A question arises as to how can the best use be made of the simulations and projections made by the current generation of CCMs, given known biases.

Figure 7a shows the October average of the fraction of the dynamical vortex covered by the 220 DU ozone contour. Note, the model time series are calculated by dividing the equivalent latitude of the 220DU contour by the equivalent latitude of the inner vortex edge derived from the individual models (see Table 2). Only E39C results are

shown in this section because E39C-A output was only available from 1990 to 1999 and therefore cannot be used to show the onset and growth of the ozone hole.

As seen in Fig. 2, the size of the observed ozone hole (defined by the 220 DU contour) grows from 1980 to 1990 and then remains relatively stable with the 220 DU contour tracking the inner vortex edge reasonably closely from 1990 to 2005. This is evident in Fig. 7a as the relative ozone hole area from observations (black solid line) increases from 0 to 1 from 1980 to 1990 and then remains relatively close to 1 from 1990 to 2005, with the exception of 2002.

Figure 7a suggests that the models are not simulating well the onset, growth and dynamical containment of the ozone hole. The ozone hole (defined by the 220 DU contour) is present at 1980 and grows to be larger than the dynamical vortex as defined by the inner vortex edge in the majority of the models, unlike the observed ozone hole which stays dynamically confined from 1990 onwards. MAECHAM4CHEM does not produce an ozone hole until 1990 and the size of the ozone hole is significantly too small relative to the size of the vortex.

As pointed out by Eyring et al. (2007), the 220 DU total column ozone contour may not be appropriate for CCMs, given known biases in the total ozone amounts. The total column ozone biases in the 5 CCMs shown here were removed by calculating the mean October total column ozone values at the equivalent latitude of the inner vortex edge over the period 1990 to 1999. For each model the difference between this mean and 220 DU was then subtracted from the modelled ozone time series. Thus the model total column ozone at the inner vortex edge averaged from 1990 to 1999 was corrected to 220 DU. The values of the bias corrections for each model are given in Table 3.

The bias corrected time series of the relative ozone hole area is shown in Fig. 7b. The agreement between the models and observations/reanalysis is greatly improved in Fig. 7b compared to Fig. 7a. All of the CCMs simulate a reasonable onset, development and dynamical containment of the ozone hole after bias correction. SOCOL perhaps shows too early an onset although the 1980 values are not available. UMETRAC manifests too much variability compared to other models and observations/reanalysis.

ACPD
8, 20155–20192, 2008

Figure 7b demonstrates that by acknowledging the known biases in CCMs, useful information in the model output can be highlighted and exploited. Figure 7b suggests that all of the models considered here capture reasonably well the onset, development and dynamical containment of the severe ozone depletion within the Antarctic polar vortex. Further, the projection of the MAECHAM4CHEM model indicates that the size of the ozone hole will be controlled by the dynamical containment of ozone depleted air until at least 2020.

6 Conclusions

The following are the primary conclusions from the study of satellite ozone measurements and the Antarctic polar vortex edge as represented in NCEP/NCAR reanalyses (Sect. 4).

- The strength of the meridional mixing barrier at the vortex edge, represented by the peak in κ, from NCEP/NCAR reanalyses steadily increased from 1980 to 2000. The 2001 to 2005 average κ peak was lower than the previous five year average but was strongly affected by the 2002 Antarctic sudden stratospheric warming.
- The equivalent latitude position of the edge of the dynamical vortex and the inner vortex edge, and therefore the size of the dynamical vortex did not change over period 1980 to 2005.
- The area of severe ozone depletion over Antarctica has been confined by the mixing barrier at the edge of the dynamical vortex since 1990.

These conclusions are consistent with the original study of B2002. An important conclusion from these results is that the position of the edge of the dynamical vortex is insensitive to the concentration of ozone within the vortex. Significant reductions in the ozone concentration inside the vortex occurred from 1980 to 1990 without any

concomitant change in the position of the vortex edge. This is supported by the CCM results shown here. In agreement with results from reanalysis, the position of the vortex edge in the five CCMs is insensitive to the concentration of ozone within the vortex. Furthermore, the MAECHAM4CHEM and SOCOL models use the same underlying GCM. The configuration of the GCM in these two models is almost identical (the non-orographic GWD schemes are tuned slightly differently) and they produce similar κ zonal means, even though the ozone distributions in the two models are very different.

It seems likely that the representation of gravity wave initiation, propagation and breaking is critical to the simulation of the Antarctic vortex in CCMs and their underlying GCMs. Holton (1983) showed that the zonal-mean wind structure of the middle atmosphere arises largely from a balance between radiative driving and gravity wave drag (GWD). Further sensitivity studies using GCMs are required to determine the particular model parameters influencing the shape of the κ peak. Although the GWD parameterizations and their interaction with the mean flow are model specific, a better understanding of what model parameters influence the representation of the vortex edge provides a pathway to improving the representation of the dynamical vortex edge in these models.

Eyring et al. (2005) point out that the validation of CCMs is best achieved using a process oriented approach, comparing CCM simulations of past stratospheric change with observations. How well CCMs simulate the dynamical barrier at the vortex edge should be considered when validating models, in particular when attempting to attribute differences between observation and model results to particular processes. For example, what may appear to be a transport problem across the vortex edge in a CCM may be resulting from a poor dynamical representation of the vortex edge. It is also important to be aware how CCMs simulate the dynamical vortex edge when making comparisons between CCM results and measurements near the edge of the Antarctic vortex or for diagnostics that depend on the area of the dynamical vortex, e.g. average daily ozone mass deficit and maximum ozone hole area (Bodeker et al., 2005) and the volume or area over which polar stratospheric clouds form. Accounting for known

biases in the representation of the dynamics and chemistry in models can highlight the useful information contained in model simulations.

Acknowledgements. We would like to thank D. Smale (NIWA) for the SOCOL and H. Garny (DLR) for the E39C-A output used in this study. The LMDz-REPRO, MAECHAM4CHEM and the DLR group acknowledges the support of the SCOUT-O3 Integrated Project which is funded by the European Commission. H. S. would like to acknowledge the NIWA high performance computing facility for their support in completing the UMETRAC simulations used in this work. The CCM SOCOL development was supported by the ETH Poly-Projects "VSGC I and II" and by the Swiss National Science Foundation (grant SCOPES IB7320-110884). This work was supported by the New Zealand Foundation for Research, Science and Technology under contract C01X0703.

References

Allen, D. R. and Nakamura, N.: A seasonal climatology of effective diffusivity in the stratosphere, J. Geophys. Res., 106(D8), 7917–7935, 2001. 20159

Andrews, A. E., Boering, K. A., Daube, B. C., Wofsy, S. C., Loewenstein, M., Jost, H., Podolske, J. R., Webster, C. R., Herman, R. L., Scott, D. C., Flesch, G. J., Moyer, E. J., Elkins, J. W. Dutton, G. S., Hurst, D. F., Moore, F. L., Ray, E. A., Romashkin, P. A., and Strahan S. E.: Mean ages of stratospheric air derived from in situ observations of CO_2, CH_4, and N_2O, J. Geophys. Res., 106(D23), 32 295–32 314, doi:10.1029/2001JD000465, 2001. 20171

Austin, J.: A three-dimensional coupled chemistry-climate model simulation of past stratospheric trends, J. Atmos. Sci., 59, 218–232, 2002. 20162

Austin, J. and Wilson, R. J.: Ensemble simulations of the decline and recovery of stratospheric ozone, J. Geophys. Res., 111, D16314, doi:10.1029/2005JD006907, 2006. 20158, 20162

Austin, J., Tourpali, K., Rozanov, E., Akiyoshi, H., Bekki, S., Bodeker, G., Brühl, C., Butchart, N., Chipperfield, M., Deushi, M., Fomichev, V. I., Giorgetta, M. A., Gray, L., Kodera, K, Lott, F., Manzini, E., Marsh, D., Matthes, K., Nagashima, T., Shibata, K., Stolarski, R. S., Struthers, H., and Tian W.: Coupled chemistry climate model simulations of the solar cycle in ozone and temperature, J. Geophys. Res., 113, D11306, doi:10.1029/2007JD009391, 2008. 20161, 20162

Bodeker, G. E., Struthers, H. A., and Connor, B. J.: Dynamical Containment of Antarctic Ozone Depletion, Geophys. Res. Lett., 29, 1098, doi:10.1029/2001GL014206, 2002. 20159, 20164
Bodeker, G. E., Shiona, H., and Eskes, H.: Indicators of Antarctic ozone depletion, Atmos. Chem. Phys., 5, 2603–2615, 2005, http://www.atmos-chem-phys.net/5/2603/2005/. 20160, 20161, 20163, 20168, 20174
Bodeker, G. E., and Waugh, D. W., Akiyoshi, H., Braesicke, P., Eyring, V., Fahey, D. W., Manzini, E., Newchurch, M. J., Portmann, R. W., Robock, A., Shine, K. P., Steinbrecht, W., and Weatherhead, E. C.: The ozone layer in the 21st century, Chapter 6 in Scientific Assessment of Ozone Depletion: 2006, Global Ozone Research and Monitoring Project, Report No. 50, 572 pp., Geneva, Switzerland, 2007. 20161, 20162
Bowman, K. P.: Large-scale isentropic mixing properties of the Antarctic polar vortex from analyzed winds, J. Geophys. Res., 98(D12), 23 013–23 027, 1993. 20159
Butchart, N., Scaife, A. A., Bourqui, M., de Grandpré, J., Hare, S. H. E., Kettleborough, J., Langematz, U., Manzini, E., Sassi, F., Shibata, K., Shindell, D., and Sigmond, M.: Simulations of anthropogenic change in the strength of the Brewer-Dobson circulation, Clim. Dynam., 27, 727–741, doi:10.1007/s00382-006-0162-4, 2006. 20164
Chen, P.: The permeability of the Antarctic vortex edge, J. Geophys. Res., 99(D10), 20 563–20 571, 1994. 20159
Chipperfield, M. P. and Feng, W.: Comment on: Stratospheric Ozone Depletion at northern mid-latitudes in the 21st century: The importance of future concentrations of greenhouse gases nitrous oxide and methane, Geophys. Res. Lett. 30(7), 1389, doi:10.1029/2002GL016353, 2003. 20157
Chipperfield, M. P., and Randel, W. J., Bodeker, G. E., Dameris, M., Fioletov, V. E., Friedl, R. R., Harris, N. R. P., Logan, J. A., McPeters, R. D., Muthama, N. J., Peter, T., Shepherd, T. G., Shine, K. P., Solomon, S., Thomason, L. W., and Zawodny, J. W.: Global Ozone: Past and Future, Chapter 4 in Scientific Assessment of Ozone Depletion: 2002, Global Ozone Research and Monitoring Project, Tech. Rep. Report No. 47, Geneva, Switzerland, 2003. 20157
Cullen, M. and Davies, T.: Conservative split-explicit integration scheme with fourth-order horizontal advection, Q. J. R. Meteorol. Soc., 117, 993–1002, 1991.
Dameris, M., Grewe, V., Ponater, M., Decker, R., Eyring, V., Mager, F., Matthes, S., Schnadt, C., Stenke, A., Steil, B., Brühl, C., and Giorgetta, M. A.: Long-term changes and variability in a transient simulation with a chemistry-climate model employing realistic forcings, Atmos.

Chem. Phys., 5, 2121-2145, 2005, http://www.atmos-chem-phys.net/5/2121/2005/. 20161

Dameris, M., Matthes, S., Deckert, R., Grewe, V., and Ponater, M.: Solar cycle effect delays onset of ozone recovery, Geophys. Res. Lett., 33, L03806, doi:10.1029/2005GL024741, 2006. 20162

Egorova, T., Rozanov, E., Zubov, V., Manzini, E., Schmutz, W., and Peter, T.: Chemistry-climate model SOCOL: A validation of the present day climatology, Atmos. Chem. Phys., 5, 1557–1576, 2005, http://www.atmos-chem-phys.net/5/1557/2005/. 20159

Eyring, V., Harris, N. R. P., Rex, M., Shepherd, T. G., Fahey, D. W., Amanatidis, G. T., Austin, J., Chipperfield, M. P., Dameris, M., Forster, P. M., Gettelman, A., Graf, H-F., Nagashima, T., Newman, P. A., Pawson, S., Prather, M. J., Pyle, J. A., Salawitch, R. J., Santer, B. D., and Waugh, D. W.: A strategy for process-oriented validation of coupled chemistry-climate models, Bull. Am. Meteorol. Soc., 86, 1117–1133, 2005. 20158, 20174

Eyring, V., Butchart, N., Waugh, D. W., Akiyoshi, H., Austin, J., Bekki, S., Bodeker, G. E., Boville, B. A., Brühl, C., Chipperfield, M. P., Cordero, E., Dameris, M., Deushi, M., Fioletov, V. E., Frith, S. M., Garcia, R. R., Gettelman, A., Giorgetta, M. A., Grewe, V., Jourdain, L., Kinnison, D. E., Mancini, E., Manzini, E., Marchand, M., Marsh, D. R., Nagashima, T., Newman, P. A., Nielsen, J. E., Pawson, S., Pitari, G., Plummer, D. A., Rozanov, E., Schraner, M., Shepherd, T. G., Shibata, K., Stolarski, R. S., Struthers, H., Tian, W., and Yoshiki, M: Assessment of temperature, trace species, and ozone in chemistry-climate model simulations of the recent past, J. Geophys. Res., 111, D22308, doi:10.1029/2006JD007327, 2006. 20161, 20162, 20169

Eyring, V., Waugh, D. W., Bodeker, G. E., Cordero, E., Akiyoshi, H., Austin, J., Beagley, S. R., Boville, B. A., Braesicke, P., Brühl, C., Butchart, N., Chipperfield, M. P., Dameris, M., Deckert, R., Deushi, M., Frith, S. M., Garcia, R. R., Gettelman, A., Giorgetta, M. A., Kinnison, D. E., Mancini, E., Manzini, E., Marsh, D. R., Matthes, S., Nagashima, T., Newman, P. A., Nielsen, J. E., Pawson, S., Pitari, G., Plummer, D. A., Rozanov, E., Schraner, M., Scinocca, J. F., Semeniuk, K., Shepherd, T. G., Shibata, K., Steil, B., Stolarski, R. S., Tian, W., and Yoshiki, M.: Multimodel projections of stratospheric ozone in the 21st century, J. Geophys. Res., 112, D16303, doi:10.1029/2006JD008332, 2007. 20158, 20161, 20162, 20169, 20172

Gettelman, A., Birner, T., Eyring, V., Akiyoshi, H., Plummer, D. A., Dameris, M., Bekki, S., Lefèvre, F., Lott, F., Brühl, C., Shibata, K., Rozanov, E., Mancini, E., Pitari, G., Struthers, H.,

Tian, W., and Kinnison, D. E.: The Tropical Tropopause Layer 1960–2100, Atmos. Chem. Phys. Discuss., 8, 1367–1413, 2008, http://www.atmos-chem-phys-discuss.net/8/1367/2008/. 20158
Gregory, D. G., Shutts, G. J., and Mitchell, J. R.: A new gravity wave drag scheme incorporating anisotropic orography and low-level wave breaking: Impact upon the climate of the UK Meteorological Office Unified Model, Q. J. R. Meteorol. Soc., 124, 463–494, 1998.
Gregory, A. R. and West, V.: The sensitivity of a models stratospheric tape recorder to the choice of advection schemes, Q. J. R. Meteorol. Soc., 128, 1827-1846, 2002.
Grewe, V.: The origin of ozone, Atmos. Chem. Phys., 6, 1495–1511, 2006, http://www.atmos-chem-phys.net/6/1495/2006/. 20170
Günther, G., Müller, R., von Hobe, M., Stroh, F, Konopka, P., and Volk, C. M.: Quantification of transport across the boundary of the lower stratospheric vortex during Arctic winter 2002/2003, Atmos. Chem. Phys., 7, 17 559–17 597, 2007, http://www.atmos-chem-phys.net/7/17559/2007/. 20159
Hassler, B., Bodeker, G. E., and Dameris, M.: Technical Note: A new global database of trace gases and aerosols from multiple sources of high vertical resolution measurements, Atmos. Chem. Phys., 8, 5403–5421, 2008, http://www.atmos-chem-phys.net/8/5403/2008/. 20171
Haynes, P. and Shuckburgh, E.: Effective diffusivity as a diagnostic of atmospheric transport 1. Stratosphere, J. Geophys. Res., 105(D18), 22 777–22 794, 2000. 20159
Hines, C. O.: Doppler-spread parameterization of gravity-wave momentum deposition in the middle atmosphere. Part 2: Broad and quasi monochromatic spectra, and implementation, J. Atmos. Sol. Terr. Phys., 59, 387–400, 1997.
Hofmann, D. J., Pyle, J. A., Austin, J., Butchart, N., Jackman, C. H., Kinnison, D. E., Lefèvre, F., Pitari, G., Shindell, D. T., Toumi, R., and von der Gathen, P.: Predicting future ozone changes and detection of recovery, Chapter 12 in Scientific Assessment of Ozone Depletion: 1998, Global Ozone Research and Monitoring Project, Tech. Rep. Report No. 44, Geneva, Switzerland, 1999. 20157
Holton J. R.: The influence of gravity wave breaking on the general circulation of the middle atmosphere, J. Atmos. Sci., 40, 2497-2507, 1983. 20174
Hoppel, K., Bevilacqua, R., Allen, D. R., Nedoluha, G. E., and Randall, C.: POAM III observations of the anomalous 2002 Antarctic ozone hole, Geophys. Res. Lett., 30(7), 1394, doi:10.1029/2003GL016899, 2003. 20163

Hourdin, F. and Armengaud, A.: The use of finite-volume methods for atmospheric advection trace species: 1. Tests of various formulations in a general circulation model, Mon. Weather Rev., 127, 822-837, 1999.
Huck, P. E., McDonald, A. J., Bodeker, G. E., and Struthers, H.: Interannual variability in Antarctic ozone depletion controlled by planetary waves and polar temperature, Geophys. Res. Lett., 32, L13819, doi:10.1029/2005GL022943, 2005. 20163, 20165
Jourdain, L., Bekki, S., Lott, F., and Lefèvre, F.: The coupled chemistry-climate model LMDz-REPROBUS: description and evaluation of a transient simulation of the period 19801999, Ann. Geophys., 26, 1391–1413, 2008, http://www.ann-geophys.net/26/1391/2008/.
Juckes, M. N. and McIntyre, M. E.: A high-resolution one-layer model of breaking planetary waves in the stratosphere, Nature, 328, 590–596, 1987. 20158
Kinnison, D. E., Brasseur, G. P., Walters, S., Garcia, R. R., Marsh, D. R., Sassi, F., Harvey, V. L., Randall, C. E., Emmons, L., Lamarque, J. F., Hess, P., Orlando, J. J., Tie, X. X., Randel, W., Pan, L. L., Gettelman, A., Granier, C., Diehl, T., Niemeier, U., and Simmons A. J.: Sensitivity of chemical tracers to meteorological parameters in the MOZART-3 chemical transport model, J. Geophys. Res., 112, D20302, doi:10.1029/2006JD007879, 2007. 20158
Kistler, R., Kalnay, E., Collins, W., Saha, S., White, G., Woollen, J., Chelliah, M., Ebisuzaki, W., Kanamitsu, M., Kousky, V., van den Dool, H., Jenne, R., and Fiorino, M.: The NCEP-NCAR 50-year reanalysis: Monthly means CD-ROM and documentation, Bull. Am. Meteorol. Soc., 82(2), 247–267, 2001. 20160
Krützmann, N. C., McDonald, A. J., and George, S. E.: Identification of mixing barriers in chemistry-climate model simulations using Rényi entropy, Geophys. Res. Lett., 35, L06806, doi:10.1029/2007GL032829, 2008. 20159
Lefèvre, F., Brasseur, G. P., Folkins, I., Smith, A. K., and Simon, P.: Chemistry of the 1991-1992 stratospheric winter: Three dimensional model simulations, J. Geophys. Res., 99, 8183–8195, 1994.
Lott, F. and Miller, M.: A new subgrid scale orographic drag parameterization; its testing in the ECMWF model, Q. J. R. Meteorol. Soc., 123, 101–127, 1997.
Lott, F., Fairhead, L., Hourdin, F., and Levan, P.: The stratospheric version of LMDz: Dynamical climatologies, arctic oscillation, and impact on the surface climate, Clim. Dyn., 25, 851–868, doi:10.1007/s00382-005-0064, 2005.
Manney, G. L., Zurek, R. W., O'Neill, A., and Swinbank, R.: On the motion of air through the

stratospheric polar vortex, J. Atmos. Sci., 51(20), 2973–2994, 1994. 20159
Manzini, E., McFarlane, N. A., and McLandress, C.: Impact of the Doppler spread parameterization on the simulation of the middle atmosphere circulation using the MA/ECHAM4 general circulation model, J. Geophys. Res., 102, 25751-25762, 1997. 20162
Manzini, E., Steil, B., Brühl, C., Georgetta, M. A., and Krüger, K.: A new interactive chemistry-climate model: 2. Sensitivity of the middle atmosphere to ozone depletion and increase in greenhouse gases and implications for recent stratospheric cooling, J. Geophys. Res., 108(D14), 4429, doi:10.1029/2002JD002977, 2003.
McFarlane, N. A.: The effect of orographically excited gravity wave drag on the general circulation of the lower stratosphere and troposphere, J. Atmos. Sci., 44, 1775–1800, 1987.
Miller, M. J., Palmer, T. N., and Swinbank, R.: Parameterization and influence subgrid-scale orography in general circulation and numerical weather prediction models, Meteorol. Atmos. Phys., 40, 84–109, 1989.
Nash, E. R., Newman, P. A., Rosenfield, J. E., and Schoeberl, M. R.: An objective determination of the polar vortex using Ertel's potential vorticity, J. Geophys. Res., 101(D5), 9471–9478, 1996. 20164
Newman, P. A., and Pyle, J. A. (lead authors) Austin, J., Braathen, G. O., Canziani, P. O., Carslaw, K. S., Forster, P. M., Godin-Beekmann, S., Knudsen, B. M., Kreher, K., Nakane, H., Pawson, S., Ramaswamy, V., Rex, M., Salawitch, R. J., Shindell, D. T., Tabazadeh, A., and Toohey, D. W.: Polar Stratospheric Ozone: Past and Future, Chapter 3 in Scientific Assessment of Ozone Depletion: 2002, Global Ozone Research and Monitoring Project, Tech. Rep. Report No. 47, Geneva, Switzerland, 2003.
Newman, P. A., Kawa, S. R., and Nash E. R.: On the size of the Antarctic ozone hole, Geophys. Res. Lett., 31(21), L21104, doi:/10.1029/2004GL020596, 2004. 20165
Newman, P. A., Daniel, J. S., Waugh, D. W., and Nash, E. R.: A new formulation of equivalent effective stratospheric chlorine (EESC), Atmos. Chem. Phys., 7, 4537–4552, 2007, http://www.atmos-chem-phys.net/7/4537/2007/.
Nishii, K. and Nakamura, H.: Tropospheric infuence on the diminished Antarctic ozone hole in September 2002, Geophys. Res. Lett., 31, L16103, doi:10.1029/2004GL019532, 2004. 20163
Paparella, F., Babiano, A., Basdevant, C., Provenzale, A. and Tanga, P.: A Largangian study of the Antarctic polar vortex, J. Geophys. Res., 102(D6), 6765–6773, 1997. 20159
Randall, C. E., Manney, G. L., Allen, D. R., Bevilacqua, R. M., Hornstein, J., Trepte, C., La-

hoz, W., Ajtic, J., and Bodeker, G. E.: Reconstruction and simulation of stratospheric ozone distributions during the 2002 Austral winter, J. Atmos. Sci., 62, 748–764, 2005. 20163

Reithmeier, C. and Sausen, R.: ATTILA: atmospheric tracer transport in a Lagrangian model, Tellus B, 54(3), 278–299, doi:10.1034/j.1600-0889.2002.01236.x, 2002. 20162

Roeckner, E., Arpe, K., Bengtsson, L., Christoph, M., Clausen, M., Dümenil, L., Esch, M., Giorgetta, M., Schlese, U., and Schulzweida, U.: The atmospheric general circulation model ECHAM-4: Model description and simulation of present-day climate, Rep. 218, Max-Planck-Inst. für Meteorol., Hamburg, Germany, 1996.

Santee, M. L., MacKenzie, I. A., Manney, G. L., Chipperfield, M. P., Bernath, P. F., Walker, K. A., Boone, C. D., Froidevaux, L., Livesey, N. J., and Waters J. W.: A study of stratospheric chlorine partitioning based on new satellite measurements and modeling, J. Geophys. Res., 113, D12307 doi:10.1029/2007JD009057, 2008. 20171

Schoeberl, M. R. and Hartmann D. L.: The dynamics of the stratospheric polar vortex and its relation to springtime ozone depletions, Science, 251, 46–51, 1991. 20158

Schraner, M., Rozanov, E., Schnadt Poberaj, C., Kenzelmann, P., Fischer, A. M., Zubov, V., Luo, B. P., Hoyle, C. R., Egorova, T., Fueglistaler, S., Brönnimann, S., Schmutz, W., and Peter, T.: Chemistry-climate model SOCOL: version 2.0 with improved transport and chemistry/microphysics schemes, Atmos. Chem. Phys. Discuss., 8, 11 103–11 147, 2008, http://www.atmos-chem-phys-discuss.net/8/11103/2008/. 20162

Sinnhuber, B. M., Weber, M., Amankwah, A., and Burrows, J.: Total ozone during the unusual Antarctic winter of 2002, Geophys. Res. Lett., 30(11), 1580, doi:10.1029/2002GL016,798, 2003. 20163

Solomon, S.: Stratospheric ozone depletion: a review of concepts and history, Rev. Geophys., 37(3), 275–316, doi:10.1029/1999RG900008, 1999. 20158, 20171

Steil, B., Brühl, C., Manzini, E., Crutzen, P. J., Lelieveld, J., Rasch, P. J., Roeckner, E., and Krüger, K.: A new interactive chemistry-climate model: 1. Present-day climatology and interannual variability of the middle atmosphere using the model and 9 years of HALOE/UARS data, J. Geophys. Res., 108(D9), 4290, doi:10.1029/2002JD002971, 2003. 20169

Stenke, A., Grewe, V., and Ponater, M.: Lagrangian transport of water vapor and cloud water in the ECHAM4 GCM and its impact on the cold bias, Clim. Dynam., 31, 491–506, doi:10.1007/s00382-007-0347-5, 2008a. 20161

Stenke, A., Dameris, M., Grewe, V., and Garny, H.: Implications of Lagrangian transport for coupled chemistry-climate simulations, Atmos. Chem. Phys. Discuss., 8, 18 727–18 764, 2008b,

http://www.atmos-chem-phys-discuss.net/8/18727/2008/. 20161
Struthers, H., Kreher, K., Austin, J., Schofield, R., Bodeker, G., Johnston, P., Shiona, H., and Thomas, A.: Past and future simulations of NO_2 from a coupled chemistry-climate model in comparison with observations, Atmos. Chem. Phys., 4, 2227–2239, 2004, http://www.atmos-chem-phys.net/4/2227/2004/.
Swinbank, R. and O'Neill, A.: A stratosphere-troposphere data assimilation system, Mon. Weather Rev., 122, 686-702, 1994. 20167
Tilmes, S., Müller, R., Grooß, J. U., Nakajima, H., and Sasano, Y.: Development of tracer relations and chemical ozone loss during the setup phase of the polar vortex, J. Geophys. Res., 111, D24S90, doi:10.1029/2005JD006726, 2006. 20159, 20164
Tilmes, S., Kinnison, D. E., Garcia, R. R., Müller, R., Sassi, F., Marsh, D. R., and Boville, B. A.: Evaluation of heterogeneous processes in the polar lower stratosphere in the Whole Atmosphere Community Climate Model, J. Geophys. Res., 112, D24301, doi:10.1029/2006JD008334, 2007. 20167
Vincent, A. P. and Tranchant, B. J. S.: Anisotropic turbulent diffusion for ozone transport at 520 K, J. Geophys. Res., 104(D22), 27 209–27 215, 1999. 20161, 20170
Warner, C. D. and McIntyre, M. E.: On the propagation and dissipation of gravity wave spectra through a realistic middle atmosphere, J. Atmos. Sci., 53, 3213–3235, 1996.
Wang, K.-Y., Hadjinicolaou, P., Carver, G. D., Shallcross, D. E., and Hall, S. M.: Generation of low particle numbers at the edge of the polar vortex, Environmental Modelling and Software, 20, 1273–1287, 2005. 20159, 20161, 20169, 20170
Williamson, D. L. and Rasch, P. J.: Water vapor transport in the NCAR CCM2, Tellus A., 46, 34–51, 1994. 20162
Zubov, V., Rozanov, E., and Schlesinger, M. E.: Hybrid scheme for three-dimensional advective transport, Mon. Wea. Rev., 127(6), 1335–1346, 1999.

Table 1. Details of the CCMs used.

	E39C-A	LMDZrepro	MAECHAM4CHEM
Underlying GCM	ECHAM4 Roeckner et al. (1996)	LMDz4 Lott et al. (2005)	MAECHAM4 Manzini et al. (1997)
# of vertical levels	39	50	39
Pressure of top model level	10hPa	0.07hPa	0.01hPa
Horizontal resolution	3.75°×3.75° (T30)	2.5°×3.75°	3.75°×3.75° (T30)
Advection	Lagrangian Reithmeier and Sausen (2002)	finite volume Hourdin and Armengaud (1999)	semi-Lagrangian Steil et al. (2003)
Orographic GWD	Miller et al. (1989)	Lott and Miller (1997)	McFarlane (1987)
non-orographic GWD	none	Hines (1997)	Hines (1997)
Reference	Dameris et al. (2005) Stenke et al. (2008b)	Lefèvre et al. (1994) Jourdain et al. (2008)	Manzini et al. (2003) Steil et al. (2003)
	SOCOL	UMETRAC	
Underlying GCM	MAECHAM4 Manzini et al. (1997)	Met Office Unified Model™ (UK) Cullen and Davies (1991)	
# of vertical levels	39	64	
Pressure of top model level	0.01hPa	0.01hPa	
Horizontal resolution	3.75°×3.75° (T30)	2.5°×3.75°	
Advection	Hybrid Zubov et al. (1999)	Eulerian (quintic-mono) Gregory and West (2002)	
Orographic GWD	McFarlane (1987)	Gregory et al. (1998)	
non-orographic GWD	Hines (1997)	Warner and McIntyre (1996)	
Reference	Egorova et al. (2005) Schraner et al. (2008)	Austin (2002) Struthers et al. (2004)	

Table 2. 10 year (1990–1999) average of the coefficients from the fitting of the first three moments to the κ zonal means. The latitude range of the fitting is listed in the last row. The uncertainty values are 1σ standard deviations of the 10 year averages of each of the fitted coefficients. A is the normalization factor. The maximum ozone gradient values are the 10 year average of the maximum of the negative gradient in total column ozone with respect to equivalent latitude (see Fig. 5).

	NCEP/NCAR	E39C-A	LMDZrepro	MAECHAM4CHEM	SOCOL	UMETRAC
A	4350±560	5760±350	7720±670	5060±340	5480±680	6600 ±1200
m_1 (vortex edge)	62.0±0.7	65.3±1.1	64.1±1.1	60.5±0.8	61.8±1.4	65.7± 2.0
m_2	4.0±0.5	9.2±0.5	8.0±0.2	5.7±0.4	5.1±0.3	6.4± 0.4
m_3	0.12±0.2	-0.09±0.1	-0.25±0.1	0.36±0.3	0.20±0.3	0.20± 0.2
Inner vortex edge	66.0	74.5	72.1	66.2	66.9	72.1
Maximum value	434	250	385	354	429	411
Max/halfwidth	46.1	11.5	20.4	26.4	35.7	27.3
Maximum ozone gradient	22.1	12.2	16.8	15.8	16.1	16.1
Latitude range of fitting	48.5–74.5	35.5–86.5	40.5–86.5	44.5–78.5	44.5–78.5	49.5– 87.7

Table 3. Total column ozone biases for the 5 CCMs. The bias was calculated relative to 220 DU at the inner vortex edge of each model averaged over 1990–1999 (see Fig. 4).

	E39C	LMDZrepro	MAECHAM4CHEM	SOCOL	UMETRAC
Total column ozone bias (DU)	–19.5	–101.5	81.5	–21.5	–67.0

ACPD
8, 20155–20192, 2008

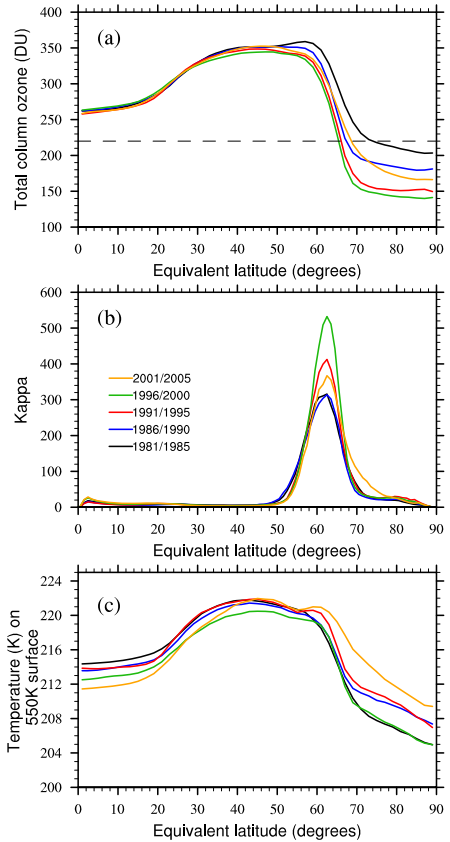

Fig. 1. Five year October averages of daily equivalent latitude zonal mean **(a)** total column ozone, **(b)** κ and **(c)** 550 K temperature from NCEP/NCAR reanalyses.

ACPD
8, 20155–20192, 2008

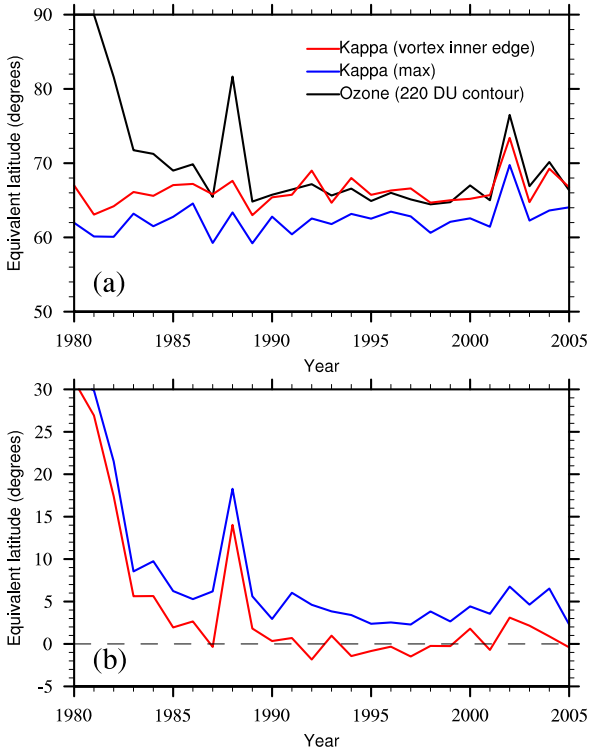

Fig. 2. **(a)** October mean equivalent latitude of the 220 DU contour (black line), the center of the vortex edge (blue line) and the inner vortex edge (red line). **(b)** Difference between the equivalent latitude of the 220 DU contour and the center of the vortex edge (blue line), and the inner vortex edge (red line). The ozone results are derived from the NIWA combined data-base and the vortex edge time series are from the NCEP/NCAR reanalyses.

ACPD
8, 20155–20192, 2008

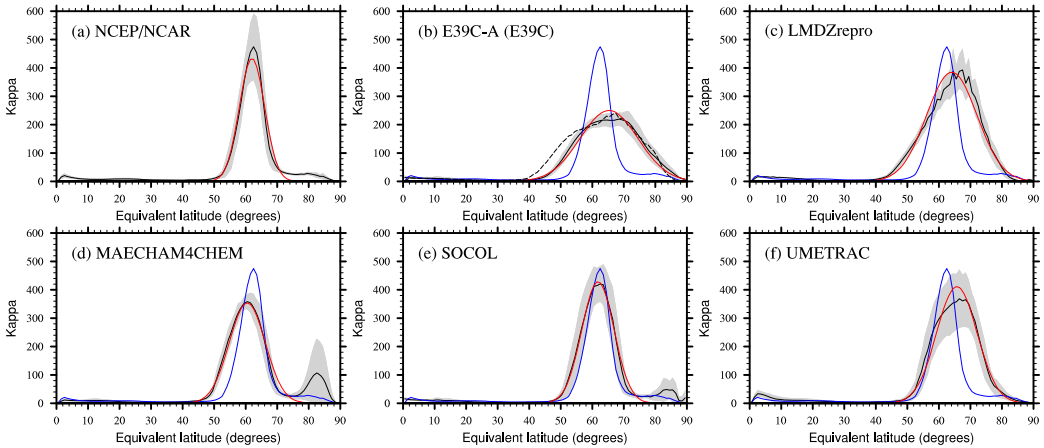

Fig. 3. 10 year (1990–1999) average October equivalent latitude zonal mean κ from **(a)** NCEP/NCAR reanalyses and **(b–f)** the five CCMs. Grey shading indicates the 1σ standard deviation about the mean. The dashed line in (b) shows results from the E39C model. The blue lines are the reanalysis mean overlaid on the model results for comparison. The red curves are the mean gaussian functions fitted to the NCEP/NCAR and modeled κ (see text for details).

ACPD
8, 20155–20192, 2008

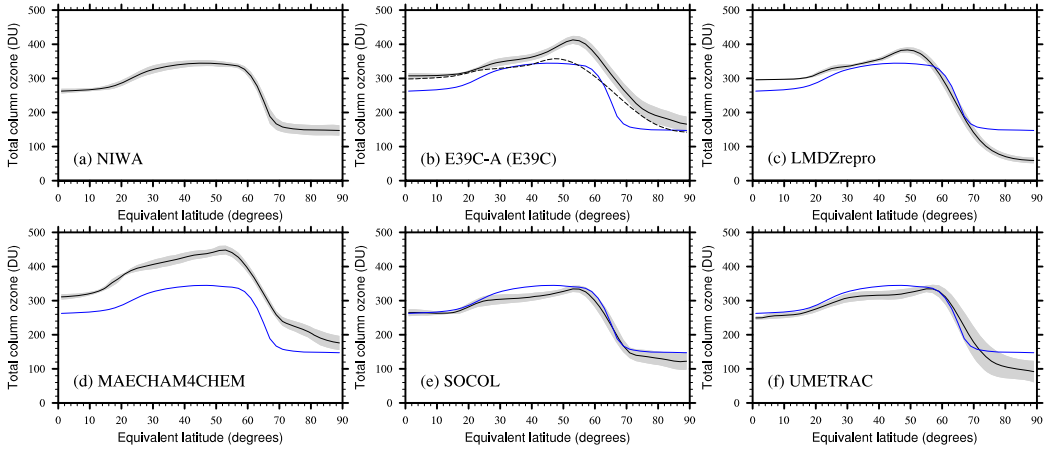

Fig. 4. 10 year (1990–1999) average October equivalent latitude zonal mean total column ozone from **(a)** NIWA combined total column ozone data-base and **(b–f)** the five CCMs. The dashed line in (b) shows results from the E39C model. Grey shading indicates the 1σ standard deviation about the mean. The blue lines are the observed mean overlaid on the model results for comparison.

ACPD
8, 20155–20192, 2008

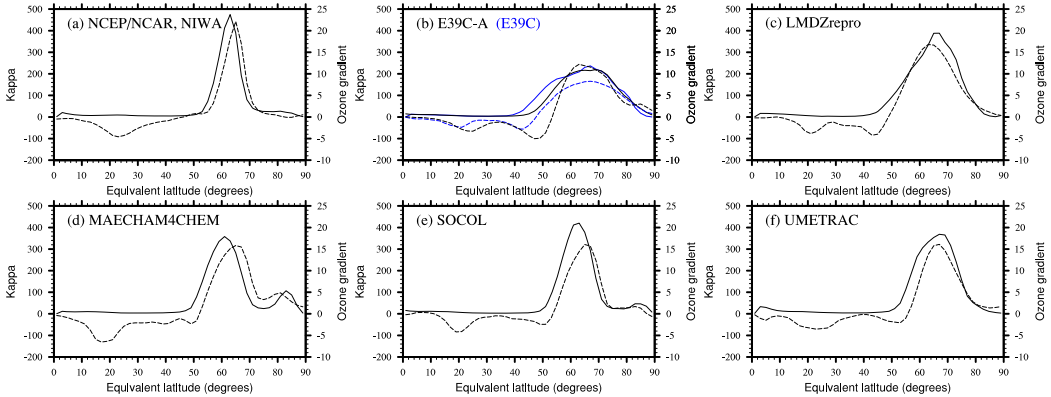

Fig. 5. Comparison of κ (solid line) and the negative of the gradient in total column ozone with respect to equivalent latitude (dashed line) from NCEP/NCAR reanalyses and NIWA observation data-base and the five CCMs. The blue lines in **(b)** shows results from the E39C model.

ACPD
8, 20155–20192, 2008

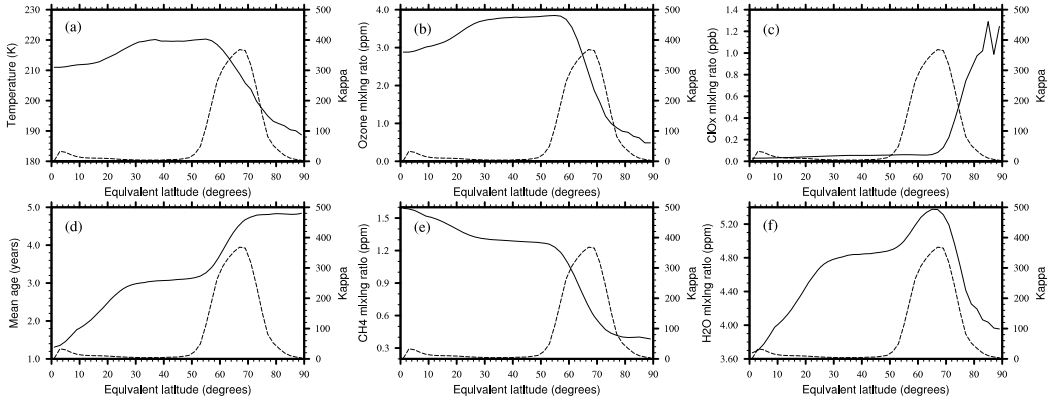

Fig. 6. UMETRAC 1990–1999 climatological October mean, equivalent latitude zonal mean temperature, trace species concentration and mean age-of-air on the 550 K potential surface. UMETRAC 550K κ (dashed lines) plotted for comparison.

ACPD
8, 20155–20192, 2008

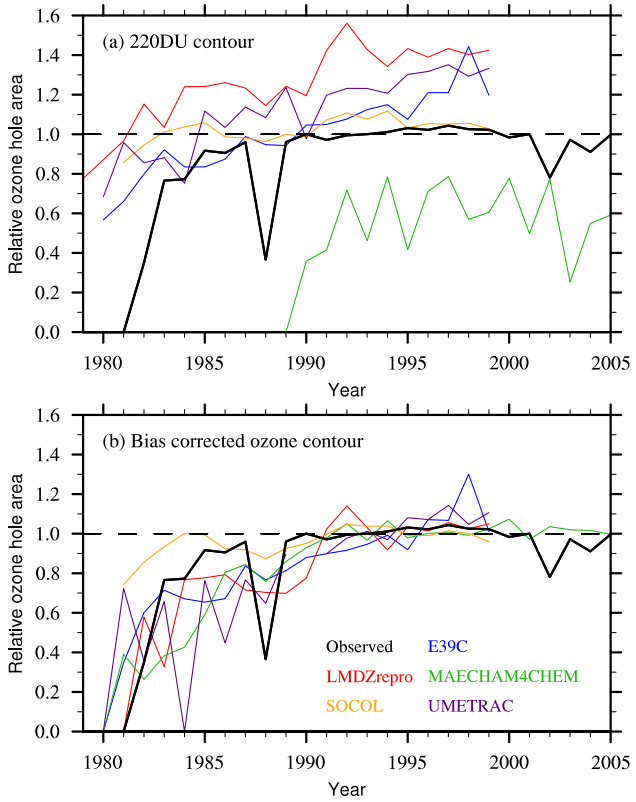

Fig. 7. Temporal evolution of the size of the ozone hole relative to the inner edge of the dynamical vortex using **(a)** the 220 DU ozone column contour to define the ozone hole, **(b)** bias corrected ozone contour values. See Table 3 for bias values and text for the definition of the biases.

ACPD
8, 20155–20192, 2008